Extended Abstract Track

Saliency Thresholds in Neural Code and its Relation to the Power-Law, Gaussian, and Lambert W Function

Anonymous *Anonymous*

Editors: List of editors' names

Abstract

The cortical neurons' response properties are peculiar in that despite the variability in the stimulus distribution the response has a stereotypic heavy-tail distribution. For example, the orientation energy model of visual cortical response results in an invariant power-law-like response distribution, regardless of the stimulus image. An interesting observation is that when this response distribution is compared with a normal (Gaussian) distribution with a matched standard deviation, the intersection where the power law distribution exceeds the matched Gaussian distribution is linearly correlated with the saliency threshold. (The same orientation energy model, when fed with a white noise image, results in a normal-distribution-like response, justifying its use as a baseline.) Further analysis reveals that this intersection point can be analytically computed using the Lambert W function, and it is also linearly correlated with the standard deviation of the response. These results point to an interesting theoretical juncture where the power law, Gaussian, and Lambert W function meets, and relates to an important threshold in neural code. In additional computational experiments, we will show how some of these results can be replicated using Recurrent Convolutional Neural Networks. These results reveal a fundamental mathematical relationship linking three ubiquitous functions in natural systems, indicating a potentially universal principle in neural computation.

Keywords: Power law, Gaussian, Lambert W function, Saliency, Neural code

1. Introduction

The cortical neurons' response distribution is quite different from that of the natural stimulus, exhibiting a stereotypical shape. For example, the neural response distribution of primary visual cortex (V1) models similar to Geisler et al. (2001) that use Gabor filtering gives a power-law-like response distribution regardless of the stimulus, while the intensity distribution of the stimuli themselves vary widely (Figure 1(c),(d)) (Lee and Choe, 2003). Recordings in Also, visual cortical neurons in the macaque exhibit sparse activity, with high kurtosis (Vinje and Gallant, 2000). These response distributions have a characteristic "heavy tail" compared to a normal (Gaussian) distribution: either lognormal, or α-stable family of distributions that include the power law (Lehky et al., 2011).

Is there a functional significance to the response level at which the response distribution becomes heavy tail, i.e., the intersection point of the response distribution and the baseline Gaussian distribution. (Figure 1(e), shows this, where the response distribution $h(E)$ is compared with the matching Gaussian $g(E)$, where E is the response level. The second intersection point is marked "L_2".) To answer this question, we will explore various computational results and theoretical open questions relating to this, most notably the relationship between power law, Gaussian, Lambert W function, and saliency thresholds in neural code.

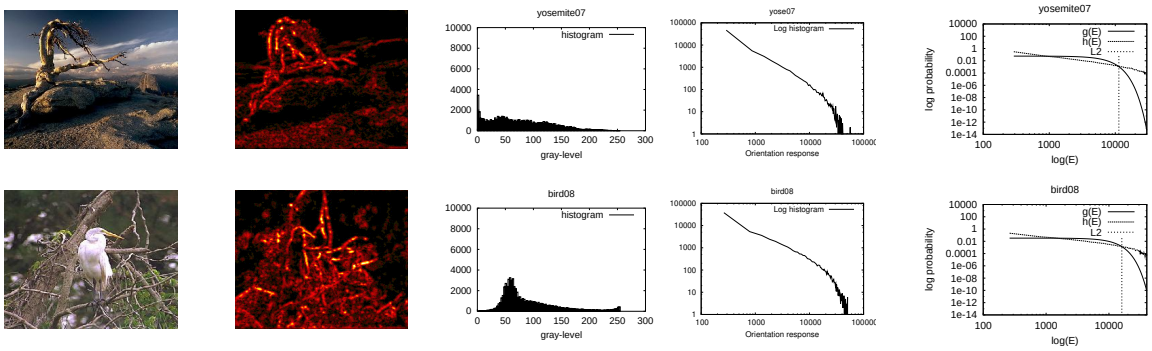

(a) Image (b) Response (c) Img. Hist. (d) Resp. Hist. (e) Resp. vs. Gaussian

Figure 1: Intensity Distribution in Images and Response Distribution in Visual Cortical Model Response. Scale: (c) linear, (d)-(e): log-log. See Sections 1 and 2 for details. Adapted from Lee and Choe (2003).

2. Background and Related Works

Lee and Choe (2003) made the first discovery of the power-law-like heavy-tail response property and its functional significance in visual cortical response models based on Geisler et al. (2001). The model was a simple series of convolutions, first with a difference-of-Gaussian to simulate the lateral geniculate nucleus, followed by orientated Gabor filters to mimic primary visual cortical response, giving E, the orientation energy.

There were three main findings in this paper: (1) the response has a power-law-like distribution (Figure 1(d)), (2) when compared to a Gaussian distribution with equal standard-deviation, the larger intersection point ('L_2' in Figure 1(e)) is linearly correlated with the saliency threshold of the response when compared to the human selected threshold (Figure 2(a))[1], and (3) the L_2 intersection point is linearly correlated with the standard deviation of the response (Figure 2(b)). In fact, it was determined that the threshold can be approximated $\theta = 1.37\sigma - 2176.69$, simply using the standard deviation of the response σ.

The Gaussian sounds like a good first approximation as a baseline, but why does it make sense as a baseline? Sarma and Choe (2006) showed that when the same visual cortical response model is presented with white-noise images, the response distribution mimics the Gaussian (similar to Figure 3(b)). This provides empirical justification, since white-noise images do not have any salient edges.

3. Further Observations with Recurrent CNN

Such power-law response we have seen above is not limited to the orientation energy model. Experiments with a biologically motivated cortical map model known as GCAL (gain con-

1. The human selected threshold was chosen by human subjects, by presenting them with 85, 90, and 95 percentile thresholded version of the response, from which the subjects picked the one with the least background noise, and the best preservation of edge features. The E value threshold was computed from these choices.

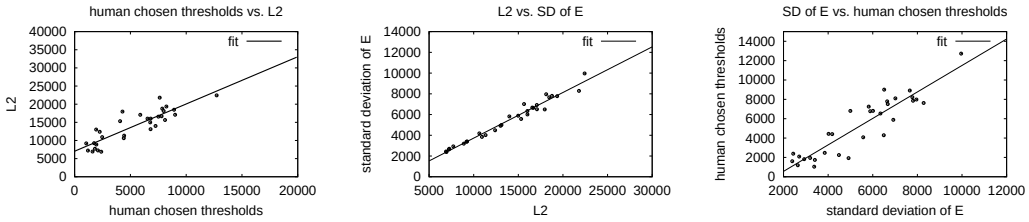

(a) Human θ vs. L_2 (b) L_2 vs. SD of E SD of E vs. Human θ

Figure 2: Relationship Among L_2, θ, and SD: L_2 = Crossover point of power law vs. Gaussian; θ = the human-selected saliency threshold of neural model response E; and SD = the standard deviation of E. Each point corresponds to one input image. Adapted from Lee and Choe (2003).

trol, adaptation, and lateral: Stevens et al. (2013)) also resulted in power-law-like response in the model trained with natural images (Park et al., 2009).

An interesting question is whether modern deep learning vision models like the Convolutional Neural Networks (LeCun et al., 1989; Krizhevsky et al., 2012) exhibit similar power-law-like response, since it is well-known that the convolution kernels in the CNN trained with natural images resemble those in V1 (Zeiler and Fergus, 2014).

The initial answer is "No", since our first attempt resulted in a Gaussian-like response distribution (cf. Figure 3(c), Loop 0). However, incorporating the lateral connections (or horizontal connections) in the visual cortex as in the GCAL model (Stevens et al., 2013), we were able to elicit a power-law response distribution using the CNN. An existing model called Recurrent CNN (RCNN: Liang and Hu (2015)) can be reinterpreted as implementing lateral connections. Using this, we conducted three experiments. The results are shown in Figure 3 (trained on CIFAR-10: see the appendix for details). Each subplot shows the change in the response based on the number of recurrent activation loops. We can see that when the network is untrained (Figure 3(a)), or when white-noise images are presented to a trained RCNN (Figure 3(b)), regardless of the number of loops, the response is Gaussian (red dashed curve). When natural images are presented to a trained RCNN, initially (Figure 3(c): Loop 0, 1) the response is close to Gaussian, but as the loop increases it approaches the power law (Figure 3(c): Loop 4, 5).

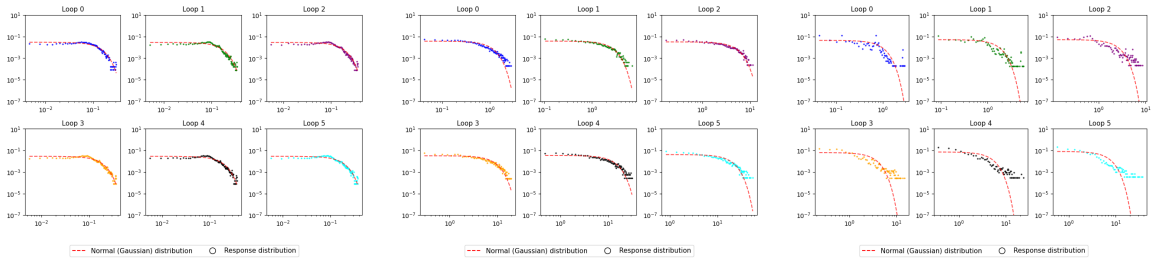

(a) Untrained/Normal Image (b) Trained/White-noise Image (c) Trained/Normal Image

Figure 3: RCNN Response Histogram (log-log). x: activity, y: frequency. See Section 3.

4. Relation to Lambert W Function and Invariance in Neural Thresholding

In an attempt to compute L_2 analytically, another ubiquitous mathematical function emerged, the Lambert W. The Lambert W function is a function $W(z)$ satisfying $W(z)e^{W(z)} = z$. Note that this is similar to $e^{ln(x)} = x$, and it can be thought of as an extended Log function: $y = e^x$ and $y = xe^x$ vs. $ln(x)$ and $W(x)$, respectively. With this, we can attempt to solve $c\frac{1}{x^a} = \frac{1}{\sigma\sqrt{2\pi}}e^{-\frac{x^2}{2\sigma^2}}$, which then gives $x = \pm\sqrt{-a\sigma^2 W\left(-\frac{(c\sigma\sqrt{2\pi})^{2/a}}{a\sigma^2}\right)}$ where c is a normalization factor, a is the power law exponent, σ = standard deviation (0 mean, and in case responses are non-negative, let it be a half normal distribution).

Just like the power law and Gaussian, the Lambert W function seems ubiquitous in science and engineering (Katsimpiri et al., 2016) with multiple applications in pure and applied mathematics, including solving transcendental equations where the unknown appears both in an exponential (such as the exponentially decaying tails of the Gaussian) and algebraically (such as the polynomially decaying tails of the power law) (Corless et al., 1996). In nature, the Lambert W emerges naturally in instances where exponential processes and polynomial processes meet (e.g., Brain oxygen/BOLD coupling, enzyme kinetics, and evolutionary models (Sotero and Iturria-Medina, 2010; Goličnik, 2010; Rocha et al., 2024; Lehtonen, 2016)). Considering known principles at play in these existing model systems and applying them to the analysis of the neural code could lead to novel insights.

Next, the observation that the intersection point L_2 is also linearly correlated with the standard deviation of the response seem to point to an invariant property regardless of the input stimulus, i.e. $\frac{\theta}{\sigma} = c$, where θ is the saliency threshold ($\sim L_2$), σ is the standard deviation, and c is some constant (empirical evidence shown in Figure 2(b)). This kind of invariance can greatly simplify downstream processing in the visual system. Furthermore, the threshold can be readily computed: Lee and Choe (2003) observed that σ can be easily computed in neural circuits, given quadratic activation functions and square root activation functions (see Boucheny et al. (2005) for models of the head direction cell that utilize these functions). An open-ended question is whether this kind of approach is universal, e.g., employed across different sensory modalities, and different levels of processing.

5. Conclusion

The contribution of this extended abstract in the context of existing works can be summarized as follows: (1) **Known result**: the relationship between power-law-like neural response and the use of the Gaussian as a baseline for saliency threshold, (2) **Known result**: linear correlation among perceptual threshold, intersection point of power-law vs. Gaussian, and standard deviation of the response, (3) **New computational results**: Recurrent CNN activity starts with Gaussian-like and progressively becomes power-law-like through the loops, and (4) **New theoretical insights**: Lambert W function provides an analytical solution for the computation of the intersection point. This leads to (5) **Open-ended questions**: deep fundamental entanglement among power-law, Gaussian, Lambert W function, and thresholds in neural code, and potential connections to criticality and self-organization in nature (Beggs, 2022).

References

John M Beggs. *The cortex and the critical point: understanding the power of emergence*. MIT Press, 2022.

Christian Boucheny, Nicolas Brunel, and Angelo Arleo. A continuous attractor network model without recurrent excitation: maintenance and integration in the head direction cell system. *Journal of computational neuroscience*, 18(2):205–227, 2005.

Robert M Corless, Gaston H Gonnet, David EG Hare, David J Jeffrey, and Donald E Knuth. On the lambert w function. *Advances in Computational mathematics*, 5(1):329–359, 1996.

W. S. Geisler, J. S. Perry, B. J. Super, and D. P. Gallogly. Edge Co-occurrence in natural images predicts contour grouping performance. *Vision Research*, 41:711–724, 2001.

Marko Goličnik. Explicit reformulations of time-dependent solution for a michaelis–menten enzyme reaction model. *Analytical biochemistry*, 406(1):94–96, 2010.

Christina Katsimpiri, Panayotis E Nastou, Panos M Pardalos, and Yannis C Stamatiou. The ubiquitous lambert function and its classes in sciences and engineering. In *Contributions in Mathematics and Engineering: In Honor of Constantin Carathéodory*, pages 323–342. Springer, 2016.

Alex Krizhevsky, Ilya Sutskever, and Geoffrey E Hinton. Imagenet classification with deep convolutional neural networks. In F. Pereira, C.J. Burges, L. Bottou, and K.Q. Weinberger, editors, *Advances in Neural Information Processing Systems*, volume 25. Curran Associates, Inc., 2012.

Yann LeCun, Bernhard Boser, John Denker, Donnie Henderson, Richard Howard, Wayne Hubbard, and Lawrence Jackel. Handwritten digit recognition with a back-propagation network. *Advances in neural information processing systems*, 2:396–404, 1989.

Hyeon-Cheol Lee and Yoonsuck Choe. Detecting salient contours using orientation energy distribution. In *Proceedings of the International Joint Conference on Neural Networks*, pages 206–211. IEEE, 2003.

Sidney R Lehky, Roozbeh Kiani, Hossein Esteky, and Keiji Tanaka. Statistics of visual responses in primate inferotemporal cortex to object stimuli. *Journal of Neurophysiology*, 106(3):1097–1117, 2011.

Jussi Lehtonen. The lambert w function in ecological and evolutionary models. *Methods in Ecology and Evolution*, 7(9):1110–1118, 2016.

Ming Liang and Xiaolin Hu. Recurrent convolutional neural network for object recognition. In *Proceedings of the IEEE conference on computer vision and pattern recognition*, pages 3367–3375, 2015.

Choonseog Park, Yoon H. Bai, and Yoonsuck Choe. Tactile or visual?: Stimulus characteristics determine receptive field type in a self-organizing map model of cortical development. In *Proceedings of the 2009 IEEE Symposium on Computational Intelligence for Multimedia Signal and Vision Processing*, pages 6–13, 2009.

J Leonel Rocha, Abdel-Kaddous Taha, and Stella Abreu. Lambert w functions in the analysis of nonlinear dynamics and bifurcations of a 2d γ-ricker population model. *Mathematics*, 12(12):1805, 2024.

Subramonia Sarma and Yoonsuck Choe. Salience in orientation-filter response measured as suspicious coincidence in natural images. In Yolanda Gil and Raymond Mooney, editors, *Proceedings of the 21st National Conference on Artificial Intelligence (AAAI 2006)*, pages 193–198, 2006.

Roberto C Sotero and Yasser Iturria-Medina. From blood oxygenation level dependent (bold) signals to brain temperature maps. *Nature Precedings*, pages 1–1, 2010.

Jean-Luc R Stevens, Judith S Law, Ján Antolík, and James A Bednar. Mechanisms for stable, robust, and adaptive development of orientation maps in the primary visual cortex. *Journal of Neuroscience*, 33(40):15747–15766, 2013.

William E Vinje and Jack L Gallant. Sparse coding and decorrelation in primary visual cortex during natural vision. *Science*, 287(5456):1273–1276, 2000.

Matthew D Zeiler and Rob Fergus. Visualizing and understanding convolutional networks. In *European conference on computer vision*, pages 818–833. Springer, 2014.

Appendix A. Methods

A.1. Computation of the Visual Cortical Response (Orientation Energy)

The visual cortical response model in Figures 1 and 2 are based on the orientation energy, defined as follows in Lee and Choe (2003).

The gray scale image I is convolved with a difference-of-Gaussian (DoG) filter D to give I_D:

$$I_D = I * D, \tag{1}$$

where $*$ is the convolution operator. D is the difference of two Gaussians $N_\sigma(x, y)$ with variance σ^2:

$$D(x, y) = N_{\sigma/2}(x, y) - N_\sigma(x, y), \tag{2}$$

$$N_\sigma(x, y) = \frac{1}{2\pi\sigma^2} \cdot exp(-\frac{x^2 + y^2}{2\sigma^2}), \tag{3}$$

where (x, y) is the pixel location.

I_D is convolved with even- and odd-phased oriented Gabor functions $G_{\theta,\phi,\sigma}(x, y)$ with orientation θ, phase ϕ, and width σ, which gives the orientation energy E for angle θ.

$$E_\theta = (G_{\theta,0,\sigma} * I_D)^2 + \left(G_{\theta,\frac{\pi}{2},\sigma} * I_D\right)^2 \tag{4}$$

$$G_{\theta,\phi,\sigma}(x, y) = exp(-\frac{x'^2 + y'^2}{2\sigma^2})cos(2\pi x' + \phi) \tag{5}$$

$$x' = xcos\theta + ysin\theta$$

$$y' = -xsin\theta + ycos\theta,$$

where (x, y) is the pixel location. The final orientation energy is the sum of these for $\theta_k = \frac{k\pi}{6}, k \in \{0, 1, 2, 3, 4, 5\}$:

$$E = \sum_{k\in\{0,1,2,3,4,5\}} E_{\theta_k}.$$

A.2. Recurrent CNN, Interpreted as the Visual Cortex with Lateral Connections

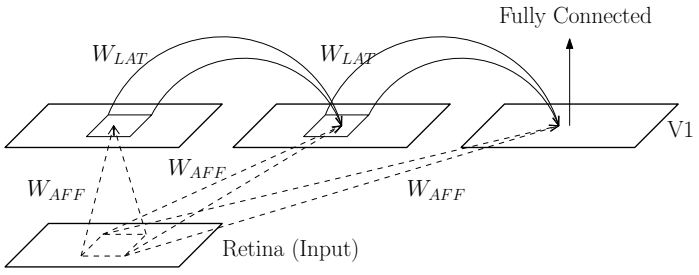

Figure 4: Recurrent CNN, Interpreted as the Primary Visual Cortex with Lateral Connections.

The Recurrent CNN by Liang and Hu (2015) uses shared feedforward weights (first conv layer weights) and recurrent weights (second conv layer weights) to iterate over the initial convolutional feature map. The recurrent activation is achieved through repeatedly activating the second conv layer through the shared weights. This can be interpreted in the context of the primary visual cortex, as shown in Figure 4. The feedforward weights correspond to the afferent weights (W_{AFF}), and the recurrent weights correspond to the lateral weights (W_{LAT}). Note that these weights are reused. Using the same W_{LAT} we can run multiple loops before sending off the featuremap activation to the fully connected layers (FC layers). Figure 4 shows Loop 1 scenario, initial activation, followed by 1 additional recurrent loop before forwarding to the FC layer. Here, Loop 0 corresponds to the feature map in the middle being forwarded to the FC layer, without additional recurrent loops.

The results in Figure 3 were obtained using this model. The two conv layers had 8 channels. The receptive field size was 7×7. The final loop was followed by max pool layer with 2×2 kernel, prior to feeding into the FC layer. We used $L1$ normalization ($\lambda = 1e-3$), and Stochastic Gradient Descent with momentum ($= 0.9$) with learning rates $\in$ {1e-2, 1e-3, 1e-4a}. Standard cross entropy loss was used. We used the CIFAR-10 data set (50k samples), with training/validation split of 85%/15%. In all cases, the images were gray-scaled, resized to 48×48. All conv layers used the ReLU function. The networks were trained for 1,000 epochs with early stopping (patience = 50).

A.3. Solving $c\frac{1}{x^a} = \frac{1}{\sigma\sqrt{2\pi}}e^{-\frac{x^2}{2\sigma^2}}$ (Sketch)

Start with

$$c\frac{1}{x^a} = \frac{1}{\sigma\sqrt{2\pi}}e^{-\frac{x^2}{2\sigma^2}}.$$

Rearrange to get

$$c\sigma\sqrt{2\pi} = x^a e^{-x^2/(2\sigma^2)}.$$

Let

$$u = \frac{x^2}{2\sigma^2},$$

and rearrange to get

$$c\sigma\sqrt{2\pi} = (2\sigma^2)^{a/2}u^{a/2}e^{-u}.$$

Isolate the $u^{a/2}$ term to the left and raise both sides to the power of $2/a$ to get

$$u = (c\sigma\sqrt{2\pi}(2\sigma^2)^{-a/2})^{2/a}e^{2u/a},$$

then multiply both sides with $e^{-2u/a}$ to get

$$ue^{-2u/a} = (c\sigma\sqrt{2\pi}(2\sigma^2)^{-a/2})^{2/a}.$$

Now we have a rough form where the Lambert W function can be applied, but we need one more step. Let

$$y = -\frac{2u}{a},$$

then

$$u = -\frac{a}{2}y,$$

and, after a few simple steps we get a form suitable for the application of the Lambert W function:

$$ye^y = -\frac{2}{a}(c\sigma\sqrt{2\pi}(2\sigma^2)^{-a/2})^{2/a}.$$

Simplifying the constants and applying the Lambert W function gives

$$y = W_k\left(-\frac{(c\sigma\sqrt{2\pi})^{2/a}}{a\sigma}\right),$$

where k identifies the branch of W (0=principal branch, -1=lower real branch). Substituting back y and u and rearranging, we get the final result:

$$x = \pm\sqrt{-a\sigma^2 W\left(-\frac{(c\sigma\sqrt{2\pi})^{2/a}}{a\sigma^2}\right)}.$$